AGU PUBLICATIONS

JGR

Journal of Geophysical Research: Oceans

RESEARCH ARTICLE

10.1002/2014JC009909

Key Points:

- Measurement uncertainties are estimated for HPLC chlorophyll concentrations and filter pad absorption data
- Propagation of measurement uncertainties into derived values of chlorophyll-specific absorption coefficients accounts for a large fraction of observed variability

Correspondence to:
D. McKee,
david.mckee@strath.ac.uk

Citation:
McKee, D., R. Röttgers, G. Neukermans, V. S. Calzado, C. Trees, M. Ampolo-Rella, C. Neil, and A. Cunningham (2014), Impact of measurement uncertainties on determination of chlorophyll-specific absorption coefficient for marine phytoplankton, *J. Geophys. Res. Oceans*, *119*, doi:10.1002/2014JC009909.

Received 14 FEB 2014
Accepted 9 DEC 2014
Accepted article online 16 DEC 2014

Impact of measurement uncertainties on determination of chlorophyll-specific absorption coefficient for marine phytoplankton

David McKee[1], Rüdiger Röttgers[2], Griet Neukermans[3], Violeta Sanjuan Calzado[4], Charles Trees[4], Marina Ampolo-Rella[4], Claire Neil[1], and Alex Cunningham[1]

[1]Department of Physics, University of Strathclyde, Glasgow, Scotland, UK, [2]Department of Remote Sensing, Helmholtz-Zentrum Geesthacht, Institute for Coastal Research, Geesthacht, Germany, [3]Marine Physical Laboratory, Scripps Institution of Oceanography, University of California, San Diego, La Jolla, California, USA, [4]Research Department, Centre for Maritime Research and Experimentation, La Spezia, Italy

Abstract Understanding variability in the chlorophyll-specific absorption of marine phytoplankton, $a_{ph}^*{}_{Chl}(\lambda)$, is essential for primary production modelling, calculation of underwater light field characteristics, and development of algorithms for remote sensing of chlorophyll concentrations. Previous field and laboratory studies have demonstrated significant apparent variability in $a_{ph}^*{}_{Chl}(\lambda)$ for natural samples and algal cultures. However, the potential impact of measurement uncertainties on derived values of $a_{ph}^*{}_{Chl}(\lambda)$ has received insufficient study. This study presents an analysis of measurement uncertainties for a data set collected in the Ligurian Sea in Spring and assesses the impact on estimates of $a_{ph}^*{}_{Chl}(\lambda)$. It is found that a large proportion of apparent variability in this set of $a_{ph}^*{}_{Chl}(\lambda)$ can be attributed to measurement errors. Application of the same analysis to the global NOMAD data set suggests that a significant fraction of variability in $a_{ph}^*{}_{Chl}(\lambda)$ may also be due to measurement errors.

1. Introduction

Material-specific inherent optical properties (IOPs) are essential components for many forward radiative transfer models and remote-sensing interpretation schemes [*Mobley*, 1994]. The chlorophyll-specific phytoplankton absorption coefficient, $a_{ph}^*{}_{Chl}(\lambda)$, is particularly important since it is used in many primary production models [*Behrenfeld and Falkowski*, 1997]. Variability in $a_{ph}^*{}_{Chl}(\lambda)$ can have a significant impact on primary productivity calculations [*Babin et al*., 1993], to the extent that some effort has been made to try to eliminate the parameter from the modeling process [*Lee et al*., 1996].

Determination of $a_{ph}^*{}_{Chl}(\lambda)$ requires measurements of two variables – the fraction of the absorption coefficient in a given water sample attributable to phytoplankton cells, $a_{ph}(\lambda)$, and the concentration of chlorophyll *a* in the sample, *Chl*. The most common methodology is to measure the absorption of particulate material retained on glass fiber filters [e.g., *Ferrari and Tassan*, 1999] before and after bleaching to determine $a_{ph}(\lambda)$ and solvent extraction of phytoplankton pigments followed by fluorometry, spectrophotometry, or high performance liquid chromatography (HPLC) to determine *Chl* [*Jeffrey et al*., 1997].

The magnitude and spectral shape of $a_{ph}(\lambda)$ is primarily determined by not only *Chl* but the pigment composition and the size of phytoplankton [*Prieur and Sathyendranath*, 1981]. Variations in $a_{ph}(\lambda)$ normalized by one of the primary photosynthetic pigments, *Chl*, reflect changes in phytoplankton taxonomy, nutritional status, photoadaptive state, and pigment packaging [e.g., *Fujiki and Taguchi*, 2002]. Phytoplankton can respond to changes in ambient light levels by rearranging pigment structures to improve photosynthetic efficiency or provide protection from potentially damaging light levels, both of which lead to changes in $a_{ph}(\lambda)$. Of special interest is the magnitude of $a_{ph}^*{}_{Chl}(\lambda)$ at a wavelength of 442 nm because at this wavelength $a_{ph}(\lambda)$ has its strongest signal. This coefficient is commonly used to assess the so-called pigment packaging effect [*Morel and Bricaud*, 1981]. The fact that observed values of the chlorophyll-specific absorption coefficient decrease with increasing *Chl* is largely driven by associated changes in phytoplankton size, with low *Chl* typically being found in clear ocean regions where picoplankton (< 2 μm diameter) dominate and high *Chl* occurring in regions where microplankton (> 20 μm diameter) make a significant contribution

[*Bricaud et al*., 1995]. This has led to development of models relating spectral absorption shape to dominant cell size [e.g., *Ciotti et al*., 2002]. Reports of large variations in measured values of $a_{ph}^{*}{}_{Chl}(\lambda)$ for natural samples are common in the literature with *Bricaud et al*. [1995] showing almost an order of magnitude variability at low *Chl*. The purpose of this paper is to quantify measurement errors for $a_{ph}(\lambda)$ and *Chl* and to examine how these errors contribute to the observed variability in $a_{ph}^{*}{}_{Chl}(\lambda)$ i.e., the spread of data around the power-law fits that are used to quantify the package effect [*Bricaud et al*., 1995].

Measurement of $a_{ph}(\lambda)$ for natural samples is subject to a number of practical limitations. As well as instrument noise and sample handling artifacts [*Stramski*, 1990], there are issues associated with separation of algal from nonalgal components of absorption [*Ferrari and Tassan*, 1999] and quantification of the path length amplification factor, β, for filter pad absorption measurements. The path length amplification factor is supposed to enable correction for diffuse reflection from the filter paper upon which the sample is retained and resulting multiple photon traversals through the sample. Various, potentially conflicting, strategies for assessing β have been proposed in the literature without any real consensus being achieved [e.g., *Mitchell*, 1990; *Bricaud and Stramski*, 1990; *Cleveland and Weidemann*, 1993; *Tassan and Ferrari*, 1995; *Arbones et al*., 1996; *Roesler*, 1998; *Finkel and Irwin*, 2001]. More recently, *Röttgers and Gehnke* [2012] have presented a new analysis of path length amplification effects and an alternative means of estimating β. One possible reason why a solution to this problem has remained elusive has been the necessity to validate the approach using absorption data measured on particle suspensions with unknown and probably significant uncertainties. In situ absorption measurements using WETLabs AC-9 instruments have been commonplace for approximately two decades, for example, but it has become clear that these data are subject to significant potential errors associated with imperfect correction for scattering artifacts [*McKee et al*., 2008; *Leymarie et al*., 2010]. Recent work has demonstrated that these issues can now be largely overcome, and typical AC-9 accuracy now approaches $\pm$ 0.02 m^{-1} [*McKee et al*., 2013].The current state of the art for total absorption measurements for natural samples is the Point Source Integrating Cavity Absorption Meter (PSICAM) proposed initially by *Kirk* [1997], and successfully implemented and validated by *Röttgers* and coworkers at the Helmholtz-Zentrum Geesthacht (HZG) [*Röttgers et al*., 2005, 2007; *Röttgers and Doerffer*, 2007]. Along with other integrated cavity absorption meter approaches [e.g., *Pope and Fry*, 1997], the PSICAM operates by placing the sample in a completely diffuse light field and measuring the loss of light due to absorption. Scattering by the sample does not affect the already diffuse light field and the technique relies upon calibration against colored solutions with known spectral absorption coefficients. The HZG instrument has been found to give $\sim$ 2% accuracy over a wide range of water conditions, with a maximum error of $\sim$ 10% for very low signal levels [*Röttgers et al*., 2005]. Unfortunately, the integrating cavity technology is currently not well suited to application of bleaching techniques to separately measure $a_{ph}(\lambda)$, so it is still necessary to perform filter pad absorption measurements. The availability of the PSICAM does, however, permit substantially less ambiguous validation of β factors for filter pad absorption data. In this paper, filter pad absorption data are compared with PSICAM results for a field study in the Ligurian Sea and estimates of uncertainties for β factors are derived.

Claustre et al. [2004] provide a thorough analysis of measurement uncertainties for HPLC *Chl* determinations made on natural samples across the Mediterranean Sea, comparing results from several groups in a round-robin exercise. The *average* agreement (*APD*—absolute percentage difference) between laboratories for this exercise was found to be as low as 5.5% for Total Chlorophyll *a* when advanced quality assurance methods were implemented. However, for the purpose of examining apparent variability in $a_{ph}^{*}{}_{Chl}(\lambda)$ for natural samples, the parameter of interest is the *range* of the relative percentage difference (*RPD*) which gives the range of uncertainty of HPLC *Chl* for any given sample. Figure 2a in *Claustre et al*. [2004] shows *RPD* values varying by $\pm$ 20% around the average value from four laboratories for each sample. It is this estimate of error range that has to be considered for the propagation of errors into the calculation of $a_{ph}^{*}{}_{Chl}(\lambda)$. *Hooker et al*. [2005] presents results from the SeaHARRE-2 intercomparison exercise involving eight laboratories and shows *APD* ranges from 4 to 20% for a dozen samples taken from the Benguela upwelling region. In this case, it is not obvious how to estimate the *RPD* uncertainty range, but given the previous results of *Claustre et al*. [2004] we can reasonably anticipate *RPD* ranges well in excess of $\pm$ 20%. *Sørensen et al*. [2007] report results of two intercomparison exercises involving 11 validation teams representing 20 laboratories. After exclusion of outliers (reported as regularly occurring and defined as being outside three standard deviations of the group median), *Sørensen et al*. [2007] found coefficients of variation (= standard deviation/median $\times$ 100) for HPLC measurements of *Chl* ranging from 10 to 25% for algal cultures, 10–16% for

Case II waters (algal and nonalgal materials contribute significantly to optical properties) and 7–40% for Case I waters (algae and covarying materials dominate optical properties). They note that prepared *Chl* extracts showed smaller uncertainties (8–15%), suggesting a significant contribution to overall uncertainty from differing filtration and extraction procedures. In order to estimate the range of uncertainty for this data set, we note that the 95% prediction interval is approximately 1.96σ, giving maximum 95% prediction interval ranges between 30 and 80% for natural samples. *Tilstone et al.* [2012] report an average percentage standard deviation of 22% for HPLC measurements of *Chl* for an intercomparison study in the North Sea involving five laboratories. Conversion to a 95% prediction interval suggests an uncertainty range of 43% for this study. Given the magnitude of these uncertainty ranges in *Chl*, and the various potential errors in $a_{ph}(\lambda)$ discussed above, there are certainly grounds for further investigation into the extent to which these errors combine to produce uncertainties in derived values of $a_{ph}^*{}_{Chl}(\lambda)$ that may be comparable to the ranges of apparent uncertainty reported for field observations.

The hypothesis tested in this paper is that considerable apparent variability in $a_{ph}^*{}_{Chl}(\lambda)$ can be attributed to measurement uncertainties in $a_{ph}(\lambda)$ and *Chl*. Data are presented from a cruise in the Ligurian Sea to establish likely boundaries for uncertainty in $a_{ph}^*{}_{Chl}(\lambda)$ determinations using the best currently available methodology. The global relevance of these findings is tested by applying reasonable uncertainty ranges for $a_{ph}(\lambda)$ and *Chl* measurements to $a_{ph}^*{}_{Chl}(\lambda)$ values reported in the NOMAD (NASA bio-Optical Marine Algorithm Data) data set [*Werdell and Bailey*, 2005].

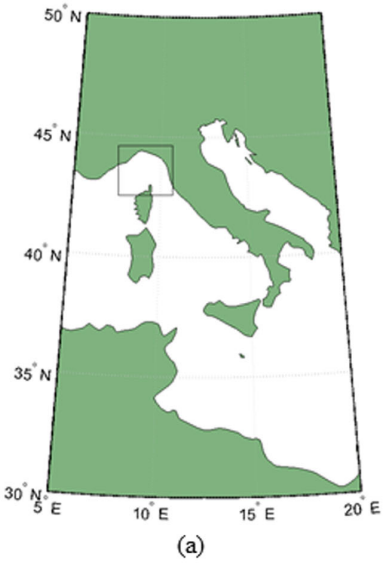

Figure 1. (a)The Ligurian Sea is located off the northwest coast of Italy in the area marked with a rectangle. (b) Location of station positions in Ligurian Sea, with offshore stations marked as circles and onshore stations marked as squares.

2. Methods

2.1. Location

Data were collected in the Ligurian Sea on board the NRV Alliance between 13th and 26th March 2009. The Ligurian Sea is located off the northwest coast of Italy (Figure 1a) and is part of the Mediterranean Sea. Stations were located in two areas: offshore and onshore (Figure 1b). The offshore group of stations represent deep (up to 2500 m) oceanic waters and at the time of the cruise were experiencing the onset of a spring bloom. Onshore stations were located close to the northwest Italian coast and consist of a series of transects across a gradient from reasonably clear water to quite turbid water associated with the plume from the River Arno. Although the data set is located within a relatively confined geographical area, it covers a reasonably wide range of optical water types. For this data set, total chlorophyll *a* concentrations ranged over an order of magnitude from 0.3 to 3.3 mg m^{-3} while total suspended particulate material concentrations varied from 0.13 to 3.8 g m^{-3}. Analysis of HPLC pigment data provided by Horn Point Laboratory suggested that microplankton dominated stations close to shore, with offshore stations typically

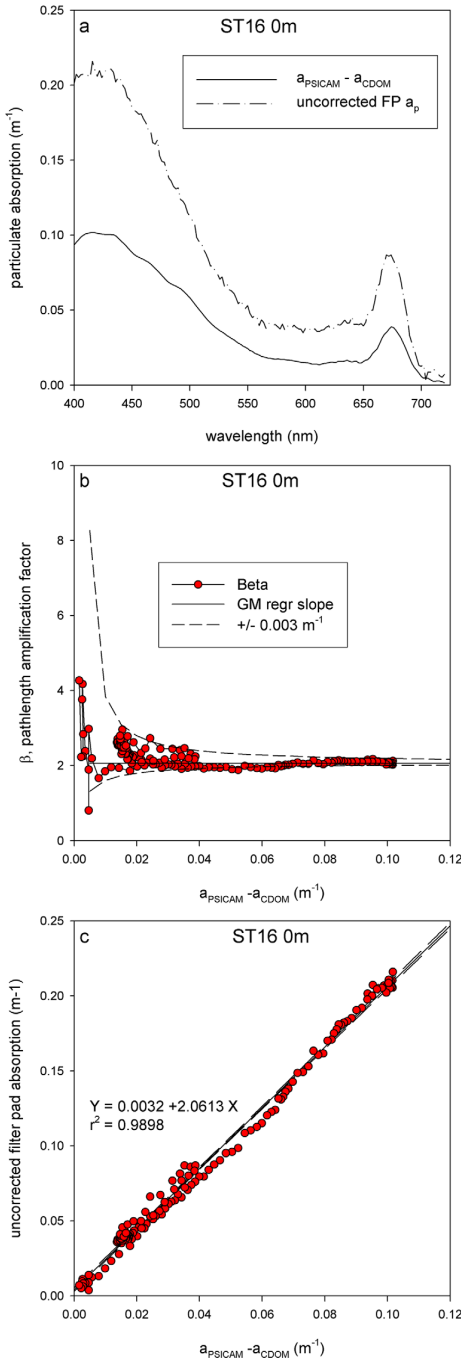

Figure 2. (a) Uncorrected filter pad absorption and corresponding "true" particulate absorption obtained by subtracting LWCC CDOM absorption from PSICAM absorption for a randomly selected single station. (b) Path length amplification factors for single sample from ratioed wavelength-dependent pairs approach suggest significant variability, particularly at low signals. (c) Geometric mean regression accounts for 99% of observed variability in the relationship between filter pad and "true" absorption. The best-fit slope is the effective, wavelength independent path length amplification factor for this sample. Dashed lines show 95% confidence intervals for the regression slope.

dominated by nanoplankton and smaller contributions from picoplankton. Samples were collected within a reasonably short time (less than 2 weeks) and only surface data are presented.

2.2. Absorption Measurements

The absorption of all dissolved and suspended components minus water was measured using the HZG PSICAM [*Röttgers et al*., 2005, 2007; *Röttgers and Doerffer*, 2007]. This instrument has previously been extensively validated and has been shown to provide very high accuracy (± 2%) absorption coefficients across a wide range of water conditions. In common with many other IOP measurement methodologies, a current limitation of the PSICAM approach is the difficulty in separating the contributions to particulate absorption of phytoplankton and of nonphytoplankton components. While it is possible to measure the absorption by colored dissolved organic materials (CDOM) using the PSICAM with 0.2 μm filtered seawater, a 1 m liquid waveguide capillary cell (LWCC) with an Ocean Optics USB2000 minispectrometer was used for the measurements presented here. This instrument is somewhat faster to operate than the PSICAM and provides noise range of ± 0.0001 m^{-1} (95% Prediction Interval) at 532 nm. In both cases, measurements were made against fresh Milli-Q references and all samples were corrected for the effects of salinity and temperature on water absorption [*Röttgers and Doerffer*, 2007]. From this pair of measurements particulate absorption, $a_p(\lambda)$, was derived by subtraction of CDOM absorption, a_{CDOM}, from PSICAM nonwater absorption, a_{PSICAM}.

In order to estimate chlorophyll-specific absorption coefficient, $a_{ph}{}^*{}_{Chl}(\lambda)$, a measurement of phytoplankton absorption, $a_{ph}(\lambda)$, is required. This can be obtained by measuring the absorption of all particulate materials retained on a GF/F filter pad, $a_p(\lambda)$, followed by measurement of the residual absorbing component after algal pigments have been eliminated by oxidation with sodium hypochlorite solution [*Ferrari and Tassan*, 1999]. The absorption measured after bleaching is commonly termed either detrital absorption, $a_{det}(\lambda)$ [*Woźniak et al*., 2010], or nonalgal absorption, $a_{NAP}(\lambda)$ [*Babin et al*., 2003]. The term $a_{det}(\lambda)$ is adopted here, even though it is noted that this absorption term contains a potentially broad range of subcomponents. Subtracting the detrital absorption signal from the particulate absorption coefficient gives the absorption associated with extracted phytoplankton pigments, which we shall refer to here as phytoplankton absorption, $a_{ph}(\lambda)$. It should be noted that the true phytoplankton absorption signal may

well differ from this value for a variety of reasons including: imperfect bleaching, absorption of the bleaching agent, presence of pigments in other particulate materials, and absorption by other, nonextractable algal materials. It is expected that phytoplankton pigments would represent the greatest fraction of algal absorption in the visible spectrum. The bleaching process may affect absorption by other organic material and could result in a tendency to underestimate detrital absorption and therefore overestimate algal absorption. This remains an area of considerable doubt and the effect, if present, would naturally vary from sample to sample. Particulate optical density (OD_p) was measured on freshly filtered samples using a Shimadzu UV-2501 PC dual-beam spectrophotometer. Between 1 and 2 L of sample were filtered through a 25 mm GF/F filter with nominal 0.7 μm retention limit which was mounted directly against the exit port of the spectrophotometer sample chamber. An unused GF/F filter, wetted with 0.2 μm filtered seawater from the same station, was used as a reference sample and mounted on the reference port of the spectrophotometer. After measuring particulate optical density, the sample filter was exposed to a dilute sodium hypochlorite solution until visual loss of pigmentation occurred. The bleached filter pad was rinsed with 0.2 μm filtered seawater before being returned to the sample detector and a further scan for detrital optical density (OD_{det}) was completed. Detrital absorption spectra were visually examined to ensure that all pigment features, including phycobiliproteins, were removed. The sample was rebleached and rescanned if necessary. The absorption coefficient is obtained from

$$a_p(\lambda) = 2.303 \frac{A_{fp} OD_p(\lambda)}{V_f \beta} \tag{1}$$

where A_{fp} is the exposed area of the filter pad, V_f is the volume of sample filtered, and β is the path length amplification factor. Filter pad absorption spectra were initially baseline corrected at 750 nm [*Cleveland and Weidemann*, 1993]. Equation (1) can be rewritten for a_{det} by replacing OD_p with OD_{det}.

One of the greatest limitations of the quantitative filter pad absorption method is determining an appropriate path length amplification factor, β. This study has the unusual benefit of having access to high-quality particulate absorption values from the combination of PSICAM and LWCC which can be used as validation data for the a_p values obtained from filter pads. Figure 2a shows a randomly selected example of an uncorrected ($\beta = 1$) filter pad particulate absorption spectrum and a corresponding PSICAM-LWCC measurement of a_p. The path length amplification factor would traditionally be calculated as the ratio of each wavelength pair of filter pad and suspension absorption coefficients, $a_{fp}(\lambda)/a_p(\lambda)$.$\beta$ values calculated in this manner for each wavelength are plotted against PSICAM-LWCC a_p in Figure 2b (for the same data set as Figure 2a), which shows increased apparent variability in β for low signal levels and is consistent with previous analyses such as *Bricaud and Stramski* [1990, their Figure 1]. Figure 2c shows a geometric mean (GM) regression [*Ricker*, 1973] applied to uncorrected filter pad absorption coefficients versus PSICAM-LWCC $a_p(\lambda)$. The regression accounts for 99% of the observed variability between these estimates of absorption and the slope provides a best-fit estimate of the path length amplification factor for the sample across all wavelengths. The uncertainty in this best-fit slope is given by 95% confidence bounds (dashed lines in figure 2c). The numerical value of this slope is plotted as a horizontal line on Figure 2b where it can be seen that β values calculated using wavelength pairs of $a_{fp}(\lambda)/a_p(\lambda)$ tend toward this best-fit slope value at high signal levels. The distribution of points around the best-fit slope value in Figure 2b is not random, but rather exhibits a systematic fluctuation in residuals about the fitted line. This was previously referred to as a "hysteresis effect" by *Bricaud and Stramski* [1990]. Residuals are higher for low signal levels ($a_{PSICAM} - a_{CDOM} < 0.04\ m^{-1}$) because of higher relative uncertainty on the absorption measurement for low signal levels. Figure 2b shows that a hypothetical error bound of $\pm 0.003\ m^{-1}$ for absorption measurements would be sufficient, in this case, to account for the vast majority of observed apparent variability in ratioed pairs β values. The boundaries for effects of measurement uncertainties were calculated using maximum and minimum values of

$$\beta_{boundary} = \frac{a'_{fp} \pm \varepsilon_a}{a_{PSICAM} - a_{CDOM} \pm \varepsilon_a} \tag{2}$$

where a'_{fp} is obtained by applying the regression equation from Figure 2c to the range of particulate absorption values, and ε_a is the hypothetical uncertainty in absorption values.

The GM regression approach outlined above was applied to each sample (i.e., a separate value of β was obtained for each sample) and was found to account for more than 90% of observed variability in over 90%

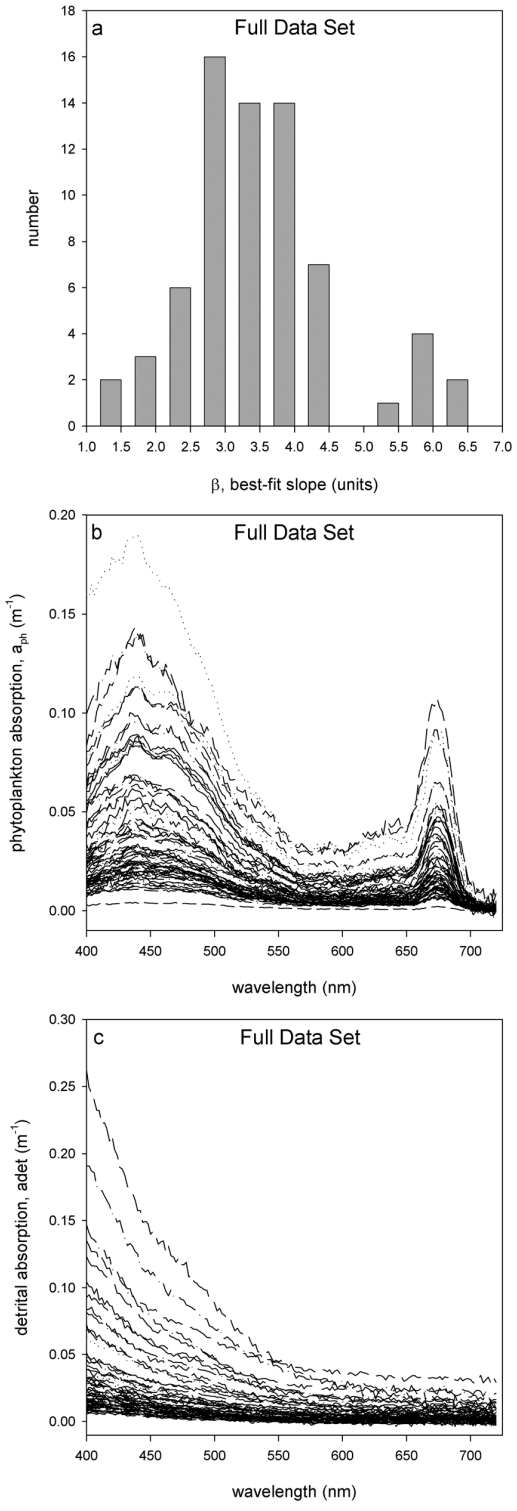

Figure 3. (a) Best-fit slopes (effective path length amplification factors) for the entire data set. Path length corrected (b) phytoplankton and (c) detrital (nonalgal particulate) spectra for surface stations in the Ligurian Sea March 2009 data set.

of cases. This approach provides a single, wavelength independent β value for each sample. An extremely wide range (~1–6.5) of best-fit slope β values was observed, as shown in Figure 3a. The median of 3.3, is considerably greater than the value of 2 predicted by *Roesler* [1998] from theoretical considerations, and the spread is well outside the range predicted by any of the previously proposed correction schemes. Best-fit GM regressions (slopes and offsets) were applied to particulate and detrital spectra, effectively assuming that the β factor is unaffected by the bleaching process. This is a necessary step that is common to all such procedures. Finally, a_{ph} was obtained by subtracting corrected a_{det} from corrected a_p. Figures 3b and 3c show resulting phytoplankton (pigment) and detrital (nonalgal particulate) absorption spectra for the entire data set. This approach (using GM offset) allows reproduction of the nonzero NIR absorption observed in PSICAM a_p spectra and attributes this to the detrital component. The filter pad absorption method we present here is conceptually similar to the traditional Transmittance (T) filter pad method, but has the distinct advantage of improved estimation of the path length amplification factor and correction for nonzero NIR absorption. It is a new method that effectively uses semiquantitative filter pad absorption measurements to partition highly accurate PSICAM particle absorption data into algal and detrital components.

2.3. Chlorophyll Measurements

Chlorophyll concentration was measured using standard HPLC measurements on samples filtered through GF/F filters, stored in liquid nitrogen, and transported to laboratories for later analysis. Two sets of data are presented here: one collected by colleagues from the Management Unit of the North Sea Mathematical Models (MUMM) and analyzed in their laboratory, and a second set collected by colleagues from NURC and analyzed by Horn Point Laboratory (HPL). Replicates for each sample were averaged by both laboratories. Samples for both labs were collected from a single CTD cast to minimize sampling error. The methodology used by HPL is given in *Hooker et al.* [2005, Chapter 5]. The HPL HPLC method uses a C8 column and a reversed phase, methanol-based, binary gradient, solvent system. The detector signal at 665 nm is used to quantify chlorophyll *a*, divinyl chlorophyll *a*, chlorophyllide *a*, pheophorbide *a*,

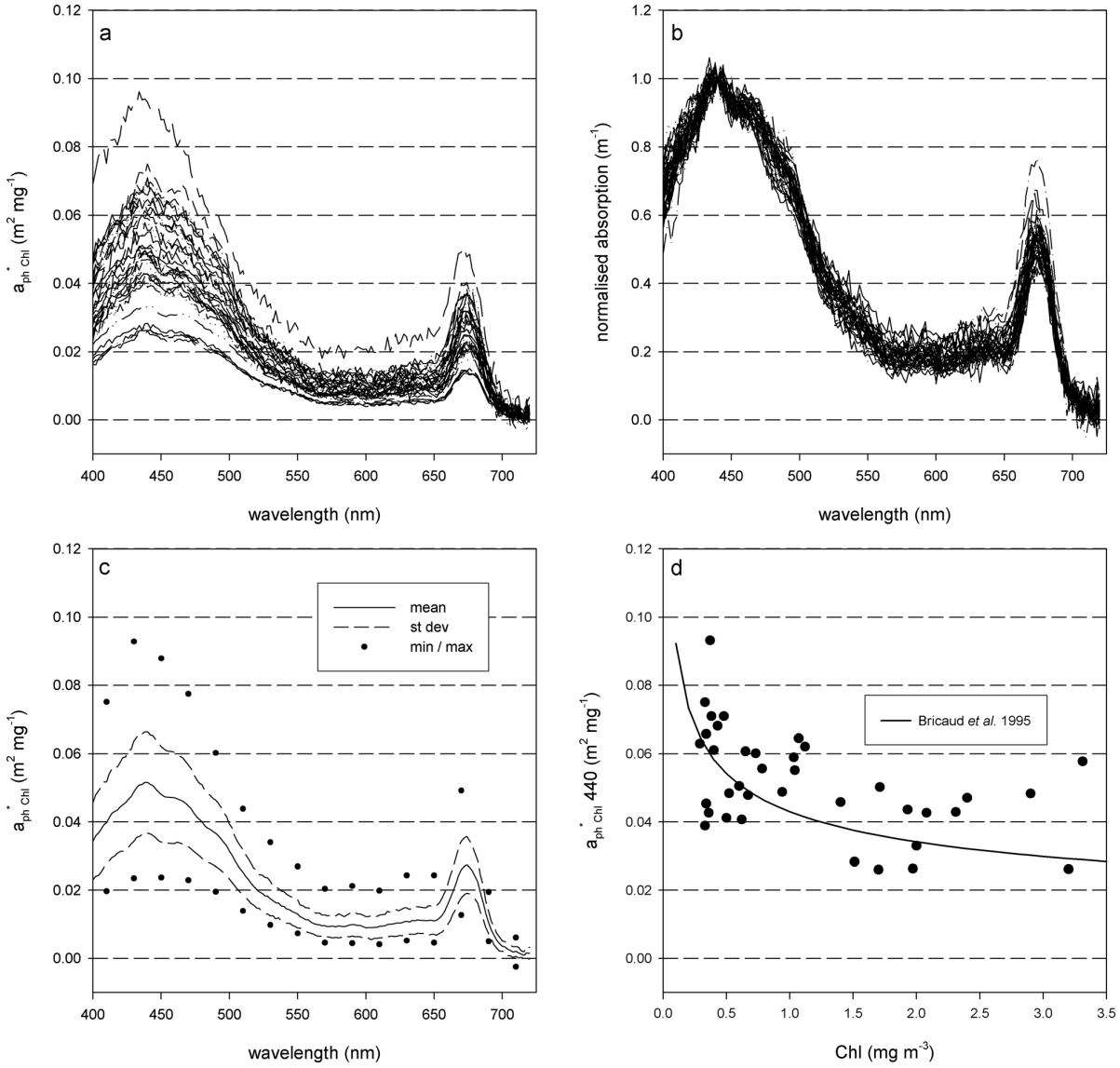

Figure 4. (a) Ratioed pairs chlorophyll-specific phytoplankton absorption spectra for the Ligurian Sea data set appear to show significant variability in magnitude, though spectral shape is reasonably self-consistent. (b) Absorption spectra normalized at 440 nm show little spectral variability across the entire data set. (c) Standard descriptive statistics highlight apparent variability in chlorophyll-specific absorption coefficient. (d) Ratioed pairs chlorophyll-specific phytoplankton absorption coefficients at 440 nm appear to generally decrease as chlorophyll concentration increases, though there is considerable spread across the entire range. The empirical relationship from *Bricaud et al.* [1995] provides a reasonable fit for this data set.

and pheophytin *a*. MUMM HPLC samples were analyzed by the Marine Chemistry Laboratory of the MUMM using a reversed phase, acetone-based method with a C18 column and a Jasco FP-1520 fluorescence detector. Total *Chl a* typically contributes ~50% of the total concentration of pigments for this data set.

3. Results

Figure 4a shows chlorophyll-specific phytoplankton absorption spectra for the entire Ligurian Sea data set (offshore and onshore) calculated by dividing each optical measurement by the corresponding chlorophyll concentration. There is an apparent order of magnitude variability in $a_{ph}{}^{*}{}_{chl}$ values at 440 nm, but little difference in spectral shape for spectra normalized to 440 nm (Figure 4b). Mean, standard deviation, and range

values for this population of spectra (Figure 4c) are consistent with other studies of this parameter [e.g., *Bricaud et al.*, 1995]. Plotting $a_{ph}^*{}_{chl}(440)$ versus *Chl* (Figure 4d) shows a general decrease toward higher concentrations that is consistent with the empirical relationship derived by *Bricaud et al.* [1995]. The data presented in Figure 4 point to a common problem: how should we interpret an apparent order of magnitude variability in $a_{ph}^*{}_{Chl}(\lambda)$? Is this real variability associated with physiological and taxonomic changes in phytoplankton populations? How much of this apparent variability in $a_{ph}^*{}_{Chl}(\lambda)$ is associated with measurement uncertainties? In order to answer these questions, it is necessary to estimate the uncertainty in $a_{ph}(\lambda)$, the uncertainty in *Chl*, and to establish how these measurement uncertainties propagate in order to quantify uncertainties in $a_{ph}^*{}_{Chl}(\lambda)$.

3.1. Uncertainty in $a_{ph}(440)$

The uncertainty in $a_{ph}(440)$ can be estimated analytically using the formula for first-order error propagation. Here it is assumed that: (a) the main sources of error are instrument noise (ΔOD) and the uncertainty in path length amplification ($\Delta\beta$), (b) these uncertainties are independent of one another, and (c) uncertainties in V_f and A_{fp} are negligible. Since

$$a_{ph} = a_p - a_{\mathrm{det}} \tag{3}$$

the uncertainty Δa_{ph} can be estimated using

$$\Delta a_{ph} = \left(\Delta a_p^2 + \Delta a_{\mathrm{det}}^2\right)^{1/2} \tag{4}$$

where

$$\Delta a_p = \left(\left(\frac{\partial a_p}{\partial OD_p}\Delta OD_p\right)^2 + \left(\frac{\partial a_p}{\partial \beta}\Delta\beta\right)^2\right)^{1/2} \tag{5}$$

Substituting equation (1) into equation (5) and differentiating gives

$$\Delta a_p = \left(\left(\frac{2.303A_{fp}}{V_f\beta}\Delta OD_p\right)^2 + \left(\frac{2.303OD_pA_{fp}}{V_f\beta^2}\Delta\beta\right)^2\right)^{1/2} \tag{6}$$

which can be rewritten as

$$\Delta a_p = \frac{2.303A_{fp}}{V_f\beta}\left(\left(\Delta OD_p\right)^2 + \left(\frac{OD_p}{\beta}\Delta\beta\right)^2\right)^{1/2} \tag{7}$$

Δa_{det} can be derived analogously by replacing OD_p by OD_{det} in equation (7). Assuming that $\Delta\beta$ is the same for the bleached and unbleached filters, then equation (4) becomes

$$\Delta a_{ph} = \frac{2.303A_{fp}}{V_f\beta}\left[\Delta OD_p^2 + \Delta OD_{\mathrm{det}}^2 + \left(\frac{\Delta\beta}{\beta}\right)^2\left(OD_p^2 + OD_{\mathrm{det}}^2\right)\right]^{1/2} \tag{8}$$

Equation (8) was used to estimate uncertainties in $a_{ph}(440)$ for each sample in the Ligurian Sea data set using recorded filtered volumes, V_f (m^3), clear filter area $A_{fp} = 4.5 \times 10^{-4}$ m^2, β values obtained from GM regressions for each filter and $\Delta\beta$ obtained from 95% confidence intervals on best-fit estimates of β. ΔOD_p and ΔOD_{det} were estimated as 95% prediction intervals ($= 1.96\ \sigma$) for OD_p and OD_{det} values between 750 and 800 nm after null correction, where it is assumed that the absorption signal is flat in this spectral region. Substituting these values into equation (8) gave a mean phytoplankton measurement uncertainty of $\Delta a_{ph}(440) = 5.8 \times 10^{-3}$ m^{-1} ($\pm$ 5.7×10^{-3} m^{-1}, 95 % Prediction Interval), which is broadly consistent with visual inspection of measured spectra. Dividing by corresponding measured values of $a_{ph}(440)$ gives a percentage error distribution that has a mean value of 13%, with a prediction interval of $\pm$ 9%.

3.2. Uncertainty in Chl

A scatter plot of HPLC *Chl* measurements from both laboratories is shown in Figure 5a. The best-fit slope of the GM regression line between both *Chl* data sets is close to unity, 0.95 $\pm$ 0.20 (95% CI), and the data sets

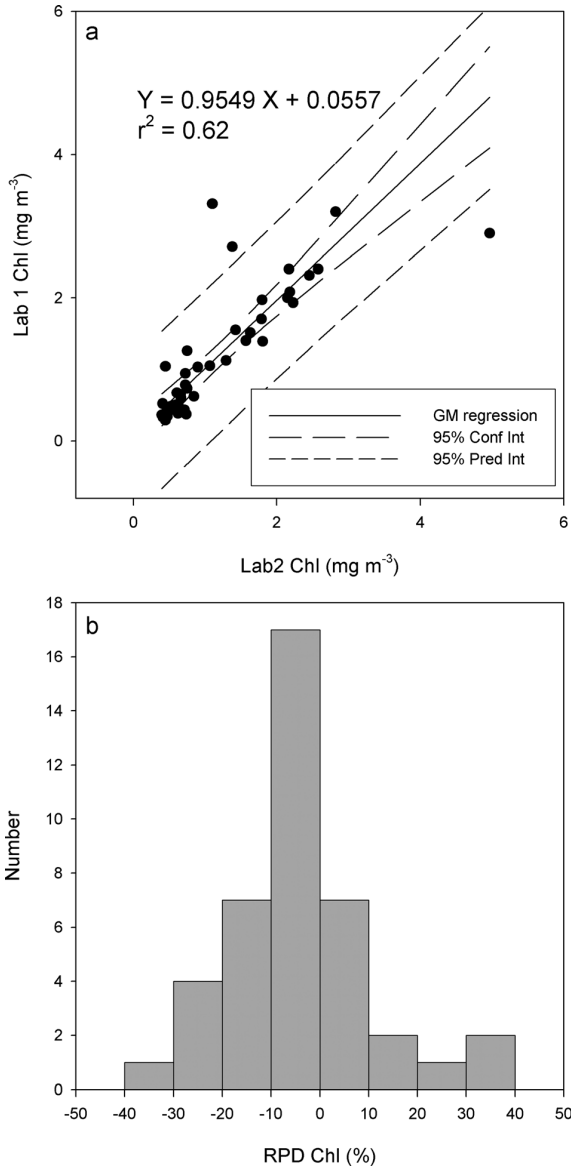

Figure 5. (a) Geometric mean regression explains 62% of observed variability between estimate of chlorophyll concentration from two different labs. (b) The Relative Percentage Difference (RPD) for chlorophyll concentration, obtained by subtracting average values from Lab 1 measured values, has a range of ± 28% (95% PI).

are well-correlated, with a correlation coefficient of 0.79 ($r^2 = 0.62$). The offset is not significantly different from zero, 0.06 ± 0.30 (95% CI). To quantify the agreement between *Chl* measurements obtained from the two laboratories, the approach of *Claustre et al*. [2004] is followed to establish *RPD* values using

$$RPD = 100\frac{Chl_i^j - \langle Chl_i \rangle}{\langle Chl_i \rangle} \quad (9)$$

where *i* represents sample number, *j* represents laboratory, and the term inside the angled brackets is the mean value of *Chl* for sample *i*. Figure 5b shows the distribution of *RPD* values for this set of *Chl* data. Using the 95% Prediction Interval to estimate the range of measurement uncertainty gives ± 28%. This is somewhat higher than the range (± 20%) found by *Claustre et al*. [2004], but is well within the ranges of uncertainty found in other studies [e.g., *Sørensen et al*., 2007; *Tilstone et al*., 2012].

3.3. Uncertainty in $a_{ph}^*{}_{Chl}$

The uncertainty in $a_{ph}^*{}_{Chl}$ can be expressed analytically as

$$\Delta a_{ph}^*{}_{Chl} = a_{ph}^*{}_{Chl}\left(\left(\frac{\Delta a_{ph}}{a_{0ph}}\right)^2 + \left(\frac{\Delta Chl}{Chl}\right)^2\right)^{1/2} \quad (10)$$

where it is assumed that the uncertainties in a_{ph} and *Chl* are not correlated. Incorporating previously derived uncertainty estimates of 21% and 28% for a_{ph} and *Chl*, respectively, into equation (10) gives an uncertainty of ±33% for $a_{ph}^*{}_{Chl}$. Figure 6a shows determinations of $a_{ph}^*{}_{Chl}$ *(440)* replotted against *Chl* for the Ligurian Sea data set. The solid line is the *Bricaud et al*. [1995] empirical best-fit for 440 nm. This has been used, together with the estimate of uncertainty in $a_{ph}^*{}_{Chl}$, to define boundaries that reflect measurement uncertainties (dashed lines). Substituting an *RPD* range of ± 20% for *Chl* [*Claustre et al*., 2004] into equation (10) gives only slightly narrower uncertainty boundaries (± 27% - dotted lines). Approximately 80% of our Ligurian Sea data set falls within the boundaries formed by these measurement uncertainty estimates.

Figure 6b shows $a_{ph}^*{}_{Chl}$ *(440)* values derived from the NOMAD data set [*Werdell and Bailey*, 2005] which includes observations from an extremely broad range of geographical locations. Following the approach of *Bricaud et al*. [1995], the least squares best-fit power law has been found for this data and estimates of uncertainty in $a_{ph}^*{}_{Chl}$ have been used to define boundaries that can be accounted for by measurement uncertainties. Sixty-three percent of NOMAD observations lie within the boundaries formed by

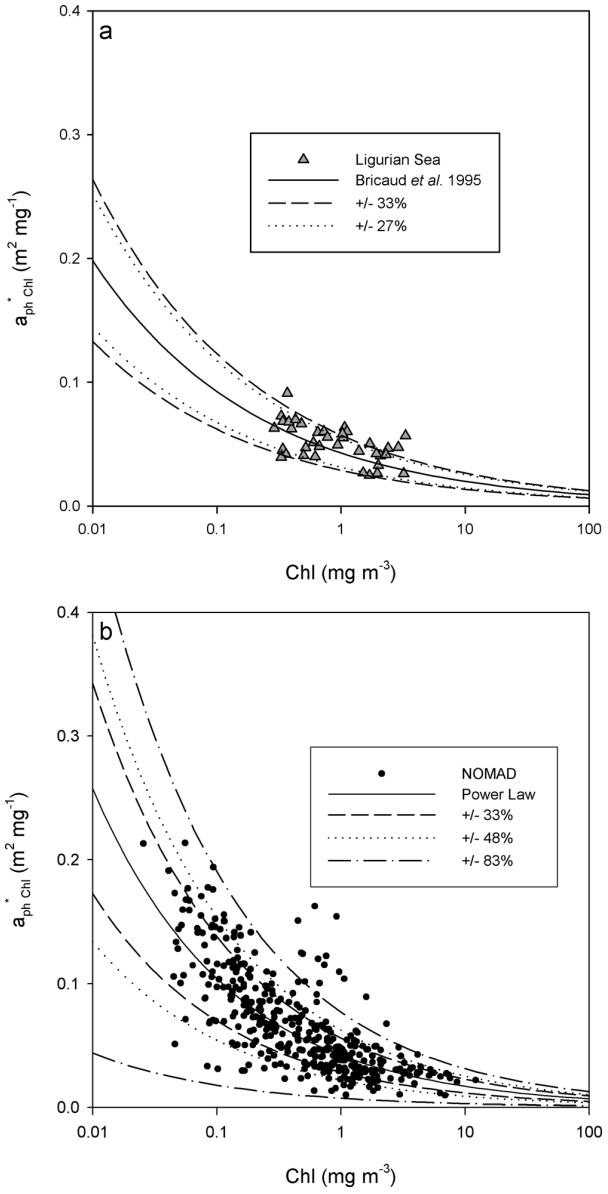

Figure 6. (a) The observed uncertainty range (± 33%) for $a_{ph}{}^*{}_{Chl}$ *(440)* for the Ligurian Sea data set (dashed lines) accounts for a large portion of the observed variability in chlorophyll-specific absorption. Reducing the uncertainty range to ± 27% (dotted lines), consistent with *Claustre et al.* [2004] uncertainties in *Chl*, provides a marginally reduced range of accounted variability in $a_{ph}{}^*{}_{Chl}$ *(440)*. (b) The Ligurian Sea chlorophyll-specific absorption data set (440 nm) is strongly consistent with the equivalent NOMAD data set. Applying the ± 33% estimated measurement uncertainty range from this study accounts for a significant fraction of the apparent variability in the NOMAD data set. Uncertainty ranges of ± 48% and ± 83%, corresponding to *Chl* uncertainty ranges derived from *Tilstone et al.* [2012] and *Sørensen et al.* [2007] respectively, greatly increases again the fraction of samples whose variability falls within the limits of measurement uncertainties.

measurement uncertainty estimates based on Ligurian Sea observations presented in this paper (± 33%). The uncertainty ranges for *Chl* measurements provided by *Sørensen et al.* [2007] and *Tilstone et al.* [2012] further increase measurement uncertainty boundaries for $a_{ph}{}^*{}_{Chl}$ (± 48% and 83%, respectively) thereby increasing the fraction of NOMAD observations (82% and 95%, respectively) located within measurement uncertainty limits. Very similar results (not shown) were found for $a_{ph}{}^*{}_{Chl}(676)$ where it is anticipated that the contribution of pigments other than *Chl* would be less than at 440 nm.

Given the very large fractions of the NOMAD $a_{ph}{}^*{}_{Chl}$ versus *Chl* data set that fall within measurement uncertainty bounds, the question arises as to how best to express uncertainty in the variability between these two parameters. If the power-law fit proposed by *Bricaud et al.* [1995] is accepted as a reasonable model for this data set (other models might also be viable e.g., *Clauset et al.* 2009], and spread around this relationship is attributed to measurement uncertainty, then the remaining uncertainty in the model can be expressed as 95% confidence intervals on the best-fit power law. Applying this to the NOMAD data set (Figure 7) gives best-fit values of 0.0456 ± 0.0031 and -0.3874 ± 0.0341 for the slope and exponent of the power law, respectively.

4. Discussion

Material-specific IOPs are the crucial link between optical measurements and concentrations of optically significant constituents that are essential for many ecosystem modelling approaches. Uncertainties in the measurement of concentrations of constituents and IOPs propagate into concentration-specific IOPs and may obscure natural variability or introduce artificial variability. It is therefore essential that these uncertainties be assessed and taken into account when discussing potential natural variability.

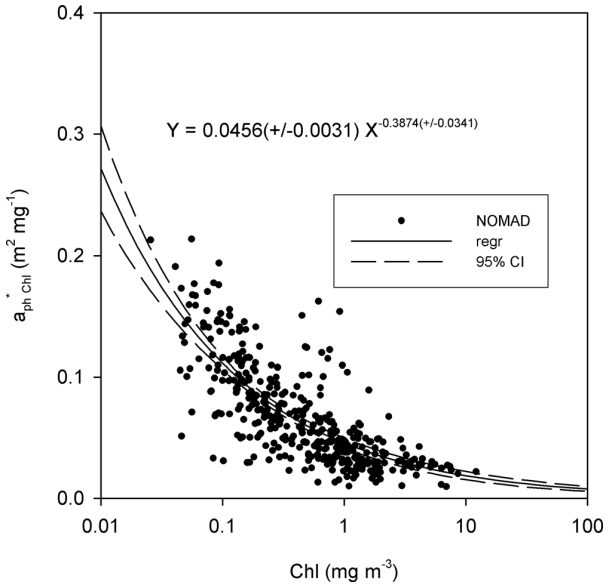

Figure 7. Using nonlinear least squares regression to fit a power law to the NOMAD data set provides slope and exponent values with associated 95% confidence intervals of 0.0456 ± 0.0031 and −0.3874 ± 0.0341, respectively. The best fit is shown as a solid line with dashed lines representing the 95% confidence interval on the regression.

In this study, both systematic and random measurement uncertainties for chlorophyll-specific phytoplankton absorption coefficients have been quantified. Systematic uncertainties in the path length amplification factor, β, are a major source of uncertainty in the measurement of the phytoplankton absorption coefficient. Access to concurrent PSICAM - LWCC derived particulate absorption data makes it possible to determine appropriate path length amplification factors for filter pad absorption data. It has been shown that β values vary widely between samples. Doubtless some of this variability will reflect the very simplistic approach of the filter pad absorption methodology used, e.g., in comparison with the *Tassan and Ferrari* [1995] approach. The excellent fit of a single regression for each set of spectral data suggests there may be artifacts associated with individual filter papers, a feature that, if true, would render prior prediction of β values impracticable. Further work is required to establish this. Of greater potential concern for this paper is the enforced assumption that the bleaching process does not impact on the β factor. While this may be a reasonable first approximation, we currently have no means of validating this approach and there must remain some associated uncertainty. This is an outstanding issue for all bleached filter pad approaches. Overall, it is reasonable to believe that this approach has eliminated potentially significant systematic errors in our filter pad particulate absorption, and that derived phytoplankton absorption coefficients will have benefited from this as well. The final value for filter pad absorption uncertainty range (± 21%) was derived using an analytical approach to error propagation, and accounts for both random and systematic measurement uncertainties.

The availability of two independent sets of *Chl* data for this cruise permits analysis of data *consistency* rather than absolute accuracy. The *RPD* range for *Chl* is a little greater than the maximum relative percentage difference reported by *Claustre et al*. [2004], but is less than the uncertainty ranges presented by two other studies [*Sørensen et al*., 2007; *Tilstone et al*., 2012]. *Claustre et al*. [2004] and *Hooker et al*. [2005] gathered leading experts in the field to determine the highest possible quality of HPLC data, whereas *Tilstone et al*. [2012] and *Sørensen et al*. [2007] might be better characterized as attempts to establish de facto standards across the broader community. In this case, the latter two sets of data are possibly more representative of the range of *Chl* uncertainties that might affect a community-sourced data set such as NOMAD.

Understanding the potential impact of measurement uncertainties on derived products such as the chlorophyll-specific absorption is essential for data interpretation. In the case of the Ligurian Sea data set examined here, a simplistic analysis of variability in $a_{ph}^*{}_{Chl}(\lambda)$ using standard descriptive statistics would suggest almost an order of magnitude variability. However, consideration of measurement uncertainties strongly suggests that the true variability in this data set is considerably less. Analysis of measurement uncertainties for the NOMAD data set suggests that much of the apparent variability in $a_{ph}^*{}_{Chl}$ for a given *Chl* concentration is also potentially attributable to measurement uncertainties.

The combination of a *Bricaud*-type curve with the error estimates from this paper is sufficient to explain the distribution of results found not only in the Ligurian Sea (Figure 6a) but also in the much wider geographical context of the NOMAD data set (Figure 6b). Our main conclusion is that published observations of $a_{ph}^*{}_{Chl}(\lambda)$ convolve an unknown degree of real variability in this parameter with a significant but

quantifiable degree of measurement uncertainty. While it would obviously be desirable to devise a means of reducing errors in measurements of $a_{ph}(\lambda)$ and *Chl*, it is essential that greater effort is made to account for the impact of measurement uncertainties on apparent variability in material-specific IOPs. Ideally, all measurements should be presented with associated estimates of uncertainty, and the analytic error propagation method described above may be used to determine uncertainties in derived products such as concentration-specific IOPs. Duplication of measurement systems on research cruises, while expensive and most often requiring close collaboration between research groups, provides vital information for uncertainty estimation rather than information redundancy.

The focus of this analysis is on the spread of data around the underlying power-law relationship that *Bricaud et al*. [1995] and others have used to describe the effect of pigment packaging on algal absorption. It seems very likely that a large fraction of this spread is associated with the propagation of measurement errors. One implication of this, is that it can therefore be assumed that there is, in fact, less natural variability in $a_{ph}^*{}_{Chl}$ than these measurements would previously have suggested. Understanding that there is less real variability in $a_{ph}^*{}_{Chl}$ than was previously thought could have implications for primary productivity modelling and development of algorithms to retrieve *Chl* from remote sensing, where adoption of reduced levels of variability around the package effect power-law relationship will significantly improve the predictive power of modeled data. For example, previously one might have taken every point in the NOMAD data set at face value and assumed that each point represents an observation of natural variability. This would have implied a massive range of variability at low *Chl* concentrations. Analysis of measurement uncertainties, however, suggests that the majority of this spread is, in fact, due to the propagation of measurement uncertainties. Given the magnitude of these uncertainty bounds, it is not possible to reliably observe variability in $a_{ph}^*{}_{Chl}$ beyond the power-law distribution that is attributed to the package effect. For further modeling activities, it is therefore reasonable to restrict variability in $a_{ph}^*{}_{Chl}$ versus *Chl* to the bounds set by the 95% confidence intervals on the power-law regression, which are much tighter than the original spread would have suggested. Of course, this must be expressed with the caveat that further natural variability might be observable if the data set is constrained to include e.g., only dark-adapted samples or samples from a single taxonomic class such as might occur in a laboratory experiment or in a carefully controlled field data set.

5. Conclusions

This study found that chlorophyll-specific absorption coefficients are significantly influenced by associated uncertainties in *Chl* and $a_{ph}(\lambda)$ measurements. While it is undoubtedly true that natural phytoplankton populations will express some degree of variability in $a_{ph}^*{}_{Chl}(\lambda)$, considerable caution should be exercised before attributing apparent variability in $a_{ph}^*{}_{Chl}(\lambda)$ to natural factors before the impact of measurement errors has been determined. The object of this paper is not to deny the existence of real variability in $a_{ph}^*{}_{Chl}(\lambda)$, but to explore the degree to which this variability can be obscured by measurement uncertainties. The fact that this analysis can be successfully applied to the NOMAD data set strongly suggests that our result is relevant on a global scale.

Acknowledgments
The authors thank Kevin Ruddick (MUMM) for providing access to HPLC data. The captain and crew of the R.V. Alliance are gratefully thanked for their professional support in the collection of this data set. Very helpful reviewers' comments were also greatly appreciated. This work was supported by the award of NERC Advanced Fellowship (NE/E013678/1) to McKee. Data to support this article are available upon request from the corresponding author (david.mckee@strath.ac.uk).

References

Arbones, B., F. G. Figueiras, and M. Zapata (1996), Determination of phytoplankton absorption coefficient in natural seawater samples: Evidence of a unique equation to correct the path-length amplification on glass-fiber filters, *Mar. Ecol. Prog. Ser.*, *137*, 293–304.

Babin, M., J.-C. Therriault, L. Legendre, and A. Condal (1993), Variations in the specific absorption coefficient for natural phytoplankton assemblages: Impact on estimates of primary production, *Limnol. Oceanogr.*, *38*, 154–177.

Babin, M., D. Stramski, G.M. Ferrari, H. Claustre, A. Bricaud, G. Obolensky, and N. Hoepffner (2003), Variations in the light absorption coefficients of phytoplankton, non-algal particles, and dissolved organic matter in coastal waters around Europe, *J. Geophys. Res.*, *108*(C7), 3211, doi:10.1029/2001JC000882.

Behrenfeld, M. J., and P. G. Falkowski (1997), A consumer's guide to phytoplankton primary productivity models, *Limnol. Oceanogr.*, *42*, 1479–1491.

Bricaud, A., and D. Stramski (1990), Spectral absorption coefficients of living phytoplankton and nonalgal biogenous matter: A comparison between the Peru upwelling area and the Sargasso Sea, *Limnol. Oceanogr.*, *35*, 562–582.

Bricaud, A., M. Babin, A. Morel, and H. Claustre (1995), Variability in the chlorophyll-specific absorption coefficient of natural phytoplankton: Analysis and parameterization, *J. Geophys. Res.*, *100*(C7), 13,321–13,332.

Ciotti, A. M., M. R. Lewis, and J. J. Cullen (2002), Assessment of the relationships between dominant cell size in natural phytoplankton communities and the spectral shape of the absorption coefficient, *Limnol. Oceanogr.*, *47*, 404–417.

Clauset, A., C. R. Shalizi, and M. E. J. Newman (2009), Power-law distributions in empirical data, *SIAM Rev.*, *51*(4), 661–703, arXiv:0706.1062 [physics.data-an], doi:10.1137/070710111.

Claustre, H., et al. (2004), An intercomparison of HPLC phytoplankton pigment methods using in situ samples: Application to remote sensing and database activities, *Mar. Chem.*, *85*, 41–61.
Cleveland, C. S., and A. D. Weidemann (1993), Quantifying absorption by aquatic particles: A multiple scattering correction for glass-fiber filters, *Limnol. Oceanogr.*, *38*, 1321–1327.
Ferrari, G. M., and S. Tassan (1999), A method using chemical oxidation to remove light absorption by phytoplankton pigments, *J. Phycol.*, *35*, 1090–1098.
Finkel, Z. V., and A. J. Irwin (2001), Light absorption by phytoplankton and the filter amplification correction: Cell size and species effects, *J. Exp. Mar. Biol. Ecol.*, *259*, 51–61.
Fujiki, T., and S. Taguchi (2002), Variability in chlorophyll a specific absorption coefficient in marine phytoplankton as a function of cell size and irradiance, *J. Plankton Res.*, *24*(9), 859–874.
Hooker, S., et al. (2005), The Second SeaWiFS HPLC Analysis Round-Robin Experiment (SeaHARRE-2), *NASA Tech. Memo. NASA/TM-2005–212785*, 112 pp., NASA Goddard Space Flight Center, Greenbelt, Md.
Jeffrey, S. W., R. F. C. Mantoura, and S. W. Wright (1997), *Phytoplankton Pigments in Oceanography: Guidelines to Modern Methods*, 661 pp., UNESCO Publ., Paris.
Kirk, J. T. O. (1997), Point-source integrating-cavity absorption meter: Theoretical principles and numerical modeling, *Appl. Opt.*, *36*, 6123–6128.
Lee, Z. P., K. L. Carder, J. Marra, R. G. Steward, and M. J. Perry (1996), Estimating primary production at depth from remote sensing, *Appl. Opt.*, *35*, 463–474.
Leymarie, E., D. Doxaran, and M. Babin (2010), Uncertainties associated to measurements of inherent optical properties in natural waters, *Appl. Opt.*, *49*, 5415–5436.
McKee D., J. Piskozub, and I. Brown (2008), Scattering error corrections for in situ absorption and attenuation measurements, *Opt. Express. 16*, 19,480–19,492.
McKee, D., J. Piskozub, R. Röttgers, and R. Reynolds (2013), Evaluation and improvement of an iterative scattering correction scheme for in situ absorption and attenuation measurements, *J. Atmos. Oceanic Tech.*, *30*, 1527–1541.
Mitchell, B. G. (1990), Algorithms for determining the absorption coefficient for aquatic particulates using the quantitative filter technique, *Proc. SPIE Int. Soc. Opt. Eng.*, *1302*, 137–148.
Morel, A., and A. Bricaud (1981), Theoretical results concerning light absorption in a discrete medium, and application to specific absorption of phytoplankton, *Deep Sea Res., Part A*, *28*, 1375–1393.
Mobley, C. D. (1994), *Light and Water, Radiative Transfer in Natural Waters*, Academic, San Diego, Calif.
Pope, R., and E. Fry (1997), Absorption spectrum (380–700 nm) of pure water. II. Integrating cavity measurements, *Appl. Opt.*, *36*, 8710–8723.
Prieur, L., and S. Sathyendranath (1981), An optical classification of coastal and oceanic waters based on the specific spectral absorption curves of phytoplankton pigments, dissolved organic matter, and other particulate materials, *Limnol. Oceanogr. 26*, 671–689.
Ricker, W. E. (1973), Linear regressions in fishery research, *J. Fish. Res. Board Can.*, *30*, 409–434.
Roesler, C. S. (1998), Theoretical and experimental approaches to improve the accuracy of particulate absorption coefficients derived from the quantitative filter technique, *Limnol. Oceanogr.*, *43*, 1649–1660.
Röttgers, R., and R. Doerffer (2007), Measurements of optical absorption by chromophoric dissolved organic matter using a point-source integrating-cavity absorption meter, *Limnol. Oceanogr. Methods*, *5*, 126–135.
Röttgers, R., and S. Gehnke (2012), Measurement of light absorption by aquatic particles: Improvement of the quantitative filter technique by use of an integrating sphere approach, *Appl. Opt.*, *51*, 1336–1351.
Röttgers, R., W. Schönfeld, P.-R. Kipp, and R. Doerffer (2005), Practical test of a point-source integrating cavity absorption meter: The performance of different collector assemblies, *Appl. Opt.*, *44*, 5549–5560.
Röttgers, R., C. Häse, and R. Doerffer (2007), Determination of the particulate absorption of microalgae using a point-source integrating-cavity absorption meter: Verification with a photometric technique, improvements for pigment bleaching and correction for chlorophyll fluorescence, *Limnol. Oceanogr. Methods*, *5*, 1–12.
Sørensen, K., M. Grung, and R. Röttgers (2007), An intercomparison of *in vitro* chlorophyll *a* determinations for MERIS level 2 data validation, *Int. J. Remote Sens.*, *28*, 537–554.
Stramski, D. (1990), Artifacts in measuring absorption spectra of phytoplankton collected on a filter, *Limnol. Oceanogr.*, *35*, 1804–1809.
Tassan, S., and G. M. Ferrari (1995), An alternative approach to absorption measurements of aquatic particles retained on filters, *Limnol. Oceanogr.*, *40*, 1358–1368.
Tilstone, G. H., et al. (2012), Variability in specific-absorption properties and their use in a semi-analytical ocean colour algorithm for MERIS in North Sea and Western English Channel Coastal Waters, *Remote Sens. Environ.*, *118*, 320–338.
Werdell, P. J., and S. W. Bailey (2005), An improved in-situ bio-optical data set for ocean color algorithm development and satellite data product validation, *Remote Sens. Environ.*, *98*, 122–140.
Woźniak, S. B., D. Stramski, M. Stramska, R. A. Reynolds, V. M. Wright, E. Y. Miksic, M. Cichocka, and A. M. Cieplak (2010), Optical variability of seawater in relation to particle concentration, composition, and size distribution in the nearshore marine environment at Imperial Beach, California, *J. Geophys. Res.*, *115*, C08027, doi:10.1029/2009JC005554.